Polymer 53 (2012) 3677–3686

Contents lists available at SciVerse ScienceDirect

Polymer

journal homepage: www.elsevier.com/locate/polymer

Synthesis of imidazolium ABA triblock copolymers for electromechanical transducers

Matthew D. Green [a], Dong Wang [b], Sean T. Hemp [c], Jae-Hong Choi [d], Karen I. Winey [d,e], James R. Heflin [b], Timothy E. Long [c,*]

[a] Department of Chemical Engineering, Macromolecules and Interfaces Institute, Virginia Tech, Blacksburg, VA 24061, USA
[b] Department of Physics, Macromolecules and Interfaces Institute, Virginia Tech, Blacksburg, VA 24061, USA
[c] Department of Chemistry, Macromolecules and Interfaces Institute, Virginia Tech, Blacksburg, VA 24061, USA
[d] Department of Materials Science and Engineering, University of Pennsylvania, Philadelphia, PA 19104, USA
[e] Department of Chemical and Biomolecular Engineering, University of Pennsylvania, Philadelphia, PA 19104, USA

ARTICLE INFO

Article history:
Received 13 March 2012
Received in revised form
8 June 2012
Accepted 13 June 2012
Available online 26 June 2012

Keywords:
Block copolymers
Ionic liquid
Actuators

ABSTRACT

Nitroxide-mediated polymerization enabled the synthesis of cationic, imidazolium-containing triblock copolymers as a membrane for an electromechanical transducer. Nitroxide-mediated polymerization afforded poly(styrene-*b*-[1-ethyl-3-(4-vinylbenzyl)imidazolium bis(trifluoromethane sulfonyl)imide)]-*b*-styrene) in a controlled fashion as confirmed using aqueous size exclusion chromatography and ^{1}H NMR spectroscopy. Dynamic mechanical analysis revealed a modulus of approximately 100 MPa for the triblock copolymer at 23 °C, which was suitable for fabrication of an electromechanical actuator. Evaluation of electromechanical actuators revealed device curvatures over twice the curvatures for Nafion® in both the presence and absence of a conductive network composite. Addition of the ionic liquid (IL) 1-ethyl-3-methylimidazolium trifluoromethane sulfonate selectively reduced the glass transition temperature (T_g) of the central block and increased overall ionic conductivity. Normalizing temperature with the central block T_g caused the ionic conductivity for the IL-incorporated polymers to collapse onto a single curve, which was an order of magnitude higher than the block copolymer in the absence of added IL.

1. Introduction

Electromechanical transducers serve as potential energy harvesting devices, biomimetic materials, and sensors [1–5]. Typical components to electromechanical transducers include a charged polymeric membrane, electrodes, and a conductive network composite (CNC) to transfer the applied potential between the electrode and the ionomeric membrane (Fig. 1) [1,6]. These devices undergo mechanical deformation (actuation) under an applied potential due to ion migration and charge accumulation inside the polymeric membrane at the membrane–electrode interface. A particularly effective CNC is an alternating layer-by-layer composite of poly(allylamine hydrochloride) and anionic gold nanoparticles. The CNC porosity effectively increases electrode surface area and improves ion transport to the electrode. The accumulation of ions at the boundary layer of the cathode increases the electro-osmotic pressure, forcing diluent or moisture into the ion-rich regions. This influx of diluent results in strain within the polymer matrix due to the swelling of the ion-rich region that macroscopically causes actuation. The diffusion of ions and diluent or moisture away from the anode causes a reduction in size of the ion-rich regions, which further facilitates actuation [1,7,8].

A critical component of the electromechanical transducer is the ionomeric membrane. Currently, Nafion® serves as a suitable control for optimal properties and response for the preparation of electrically stimulated electromechanical transducers [9]. However, recent efforts focus on the synthesis of novel ionomers with potential for preparing electroactive devices [10]. The microphase-separated morphology in Nafion® membranes assists in providing superior performance as an electromechanical transducer. The semi-crystalline perfluorinated backbone provides mechanical strength and solvent-resistance while the perfluoronated polyether side chains terminated with sulfonic acid groups phase separate into ion clusters and channels upon hydration, which enables ion conduction [11,12]. Block copolymers synthesized using controlled radical polymerization techniques present a facile strategy to mimic Nafion® through the inclusion of hard domains for mechanical reinforcement and ion-rich phases to facilitate ion

* Corresponding author. Tel.: +1 540 231 2480; fax: +1 540 231 8517.
E-mail address: telong@vt.edu (T.E. Long).

0032-3861/$ – see front matter © 2012 Elsevier Ltd. All rights reserved.
http://dx.doi.org/10.1016/j.polymer.2012.06.023

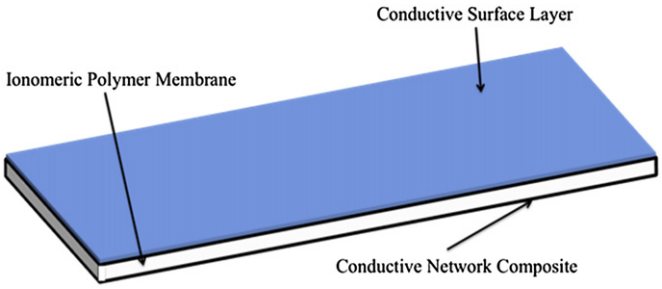

Fig. 1. Schematic of an ionomeric polymer transducer.

migration [13]. Accounts of cationic triblock copolymers for electromechanical device fabrication are currently absent in the literature. However, numerous studies focused on the optimization of thermomechanical properties, morphology, and ionic conductivity for electroactive membrane applications [14]. It is recognized that an ideal electromechanical transducer displays modest modulus (~100 MPa) and ionic conductivity (~1 mS/cm) at operation temperature, and a microphase-separated morphology promotes ion conduction in concert with mechanical ductility.

Ionic liquids (ILs) are salts with melting temperatures below 100 °C [15]. Imidazolium ILs possess a number of desirable characteristics including negligible volatility, high ionic conductivity, high thermal stability, tunable chemical structure, and wide electrochemical windows [16–20]. Earlier optimization of imidazolium IL structure focused on chemical substituents on the imidazole ring and variation of counteranions to improve properties. Tuning the substituents on the 1- and 3-positions of the imidazolium ring tailors thermal stability, viscosity, and ionic conductivity; anion selection additionally improves thermal stability and conductivity significantly while decreasing viscosity and T_g [21–23]. Large fluorinated counteranions enhance thermal stability and ionic conductivity. For example, imidazolium ILs with weakly basic counteranions such as bis(trifluoromethane sulfonyl)imide (Tf_2N^-) and trifluoromethane sulfonate (TfO^-) displayed higher thermal stability and ionic conductivity when compared to more basic counteranions such as halides [24,25].

ILs serve as diluents within ionomeric polymer transducers for several of their beneficial attributes listed above. Leo and coworkers studied IL-swollen Nafion® membranes as a method to improve performance of hydrated Nafion® [26,27]. Traditional electromechanical devices utilizing Nafion® suffer from both electrochemical reactions with water and evaporation of water during actuation. The addition of IL addressed these problems due to negligible vapor pressure and wide electrochemical window, however, slow response time remained an issue for IL-swollen Nafion®. Therefore, Leo and coworkers studied the effect of the surface area to volume ratio in the CNC of IL-incorporating actuators to improve response time for electromechanical devices. They showed a tradeoff in device performance between higher surface area to volume ratios and the electrical conductivity of the metal in the CNC [28]. Zhang and coworkers studied the impact of binding energy between the anion and imidazolium cation of the IL on actuator charging time and observed significantly shorter charging times for TfO^- versus tetrafluoroborate (BF_4^-) anions [29]. The decreased binding energy of the TfO^- anion reduced ionic cluster formation that ultimately improved the charging time. The various states of ions in imidazolium-based ILs include the free ion state, and ionic cluster states comprised of the ion pair state, the triple ion state, and the quadrupole state. Free ions contribute to ionic conductivity, and conversely ionic clusters potentially act as physical crosslinks that increase T_g and reduce ion mobility and ionic conductivity. The ratios of free ions to ionic clusters related to the binding energy of the anion as the imidazolium cation remained constant. Zhang and coworkers also studied the rate of actuation and produced strain from imidazolium IL cations and anions in Nafion® membranes [30]. They observed an ion mobility ~1.5 times larger for cations and a strain production ~4 times larger for anions.

Recent studies focused on optimizing polyelectrolyte homopolymer properties to maximize their impact on block copolymer functionality upon incorporation. Long and coworkers tailored thermal stability, T_g, and ionic conductivity of *N*-vinylimidazolium homopolymers through variation of counteranion and alkyl substituent length [31]. Additionally, Mahanthappa and coworkers investigated imidazolium homopolymers based on 1-(4-vinylbenzyl)imidazole (VBIm) and concluded that two parameters, alkyl substituent length and counteranion selection, significantly influenced ionic conductivity and thermal properties [32]. Their findings led to the design of poly(styrene-*b*-VBIm) diblock copolymers, which revealed that decreasing imidazolium block lengths shifted nanoscale lamellae morphologies to a mixture of cylinders and lamellae [33]. The ionic conductivity increased over two orders of magnitude with increasing imidazolium block lengths. Another method to improve ionic conductivity of a polymeric membrane includes IL incorporation. Lodge, Frisbie and coworkers investigated gels upon swelling two triblock copolymers, poly(styrene-*b*-ethylene oxide-*b*-styrene) and poly(styrene-*b*-methyl methacrylate-*b*-styrene), with IL and observed an increase in ionic conductivity [34]. Specifically, the IL selectively incorporated into the uncharged, polar center blocks of the triblock copolymers without a decrease of modulus.

A similar class called dielectric electromechanical transducers functions through the generation of a compressive Maxwell stress across a thermoplastic elastomer gel (TPEG) under an applied electric field [35]. Spontak and coworkers investigated several neutral triblock copolymers that selectively imbibed aliphatic mineral oil in the central block [36–42]. These triblock copolymer gels comprised of polystyrene or poly(methyl methacrylate) outer blocks and poly(*n*-butyl acrylate), poly(ethylene-*co*-butylene), or poly(ethylene-*co*-propylene) central blocks. In summary, Spontak and coworkers investigated the influence of morphology [42], composition and molecular weight [37–40], addition of non-network forming diblock copolymers [41], and sample thickness and prestrain applied [36] on the performance of dielectric electromechanical transducers. The neutral state and lack of ion diffusion under an applied electric field separate these materials from the ionic electromechanical transducers investigated herein. Their soft, gel-like nature potentially limits applications where mechanically robust materials are necessary in addition to the increased voltage required for successful operation. Finally, the incorporation of IL in cationic triblock copolymers potentially eliminates the need for added water typically required in traditional ionic electromechanical transducers.

We aimed to prepare cationic triblock copolymers that mimic the combined mechanical properties and ion conductivity of commercially available Nafion® with comparable actuator performance. A significant disadvantage associated with using commercially available polymers for electromechanical transducers is the lack of control over several polymer parameters including composition, thermomechanical properties, morphology, and molecular weight. Therefore, investigating novel imidazolium-based triblock copolymers using controlled radical polymerization allowed for targeted molecular weights and tunable compositions. Thermomechanical analysis displayed a polymer modulus suitable for electromechanical transducer fabrication [1,43,44], and actuator testing revealed superior curvature relative to Nafion®.

Analysis of the impact of added IL on the thermal properties and ionic conductivity revealed the importance of T_g and ion concentration.

2. Experimental section

4-Vinylbenzyl chloride (VBCl, Sigma, 90%), imidazole (Sigma, 99%), 1-bromoethane (Sigma, 98%), sodium bicarbonate (Sigma, ≥99.5%), sodium acetate (Sigma, ≥99%), sodium hydroxide (Sigma, ≥98%), glacial acetic acid (Sigma, ≥99%), hydrochloric acid (Sigma, 37%), 1-ethyl-3-methylimidazolium triflate (TfO) ([EMIm][TfO], IoLiTec Inc., 99%) and lithium bis(trifluoromethane sulfonyl)imide (Tf_2N) ($LiTf_2N$, Aldrich, 99%) were used as received. Styrene (Sigma, 99%) was passed over silica to remove inhibitor prior to use. Acetone (Fisher Scientific, HPLC grade), ethyl acetate (Fisher Scientific, HPLC grade), diethyl ether (Fisher Scientific, ACS grade), methanol (Fisher Scientific, HPLC grade), hexanes (Fisher Scientific, HPLC grade) and *N*,*N*-dimethylformamide (DMF, Fisher Scientific, Spectranalyzed®) were used as received. Ultrapure water was retrieved from a Virginia Water Systems, Inc. water purification system with a resistance of 17.6 MΩ DEPN and $DEPN_2$ were synthesized according to previous literature accounts [45,46].

^{1}H NMR was performed using a 400 MHz Varian Unity at 25 °C. Thermogravimetric analysis (TGA) was performed using a TA Instruments TGA 2950 at a 10 °C/min heating ramp. Differential scanning calorimetry (DSC) was performed using a TA Instruments Q1000, scans were performed under N_2 with heating at 10 °C/min and cooling at 100 °C/min, T_g's were recorded on the 2nd heating cycle. Dynamic mechanical analysis (DMA) was performed with a TA Instruments Q800 at a 3 °C/min heating ramp in film tension mode, and a single frequency of 1 Hz. Aqueous size exclusion chromatography (SEC) in a ternary mixture of water, methanol, and acetic acid (54:23:23 v/v/v%) with 0.1 M sodium acetate at 35 °C, and a flow rate of 0.8 mL/h, determined the absolute polymer weight-average molecular weights (M_w) using the refractive index detector and a multi-angle laser light scattering (MALLS) detector. Refractive index increment (d*n*/d*c*) measurements were performed using a Wyatt Optilab T-rEX equipped with a 690 nm laser at 35 °C. Poly(1-(4-vinylbenzyl)imidazole) homopolymers (1.0–5.0 mg/mL) were dissolved in the ternary mixture and injected into the dRI detector with a syringe pump. The d*n*/d*c* values were determined with the Astra V software from Wyatt, and used to determine absolute M_w from SEC. Electrochemical impedance spectroscopy (EIS) was performed using an Autloab PGSTAT 302N potientiostat and a four-point electrode sample cell purchased from BekkTeck, Inc. An applied alternating sine-wave potential was applied at 0.2 V at frequencies ranging from 1 MHz to 0.1 Hz. The temperature was controlled using an ESPEC BTL-433 environmental temperature which controlled the temperature to ±0.1 °C and 10% RH to ±0.1%. Real resistance values were taken as the high *x*-axis intercept of the Nyquist plot of imaginary impedance vs. real impedance.

Electromechanical transducers were fabricated in a two part process: the CNC coatings were fabricated using the layer-by-layer method, and then gold foil was hot pressed on the outer surface of both sides to serve as the electrode. To apply the CNC, the polymeric membrane was attached to a 1 in ×2 in polycarbonate frame using double sided tape, and mounted in an automatic dipping system (StratoSequence VI Robot, nanoStrata Inc.). To assemble each bilayer, the framed membrane was dipped into an aqueous solution of positively charged poly(allylamine hydrochloride) (PAH, 10 mM, pH = 4, Aldrich) for 3 min at 23 °C, dipped into DI water for 2 min at 23 °C three times, dipped into an anionic gold nanoparticle suspension (20 ppm, pH = 9, 3.2 nm diameter, −40 mV zeta potential, Purest Colloids Inc.) for 3 min at 23 °C, and dipped into DI water for 2 min at 23 °C three times. Electrostatic self-assembly neutralized the excess charge from the polymer or outer layer, and repeating this process produced homogeneous and even coatings with nanoscale control over thickness tailored through adjusting the number of layers. The CNC coated polymeric membrane was compression molded at 95 °C and 700 lbs for 20 s between two pieces of gold foil 50 nm in thickness to prepare the final electromechanical transducer. The actuator was cut into a 1 mm × 8 mm strip for testing, and a 4.0 V DC step voltage (HP 6218A power supply) was applied under ambient conditions (23 °C and ~43% RH) to the electromechanical transducer to analyze the bending response. Bending was recorded using a Sony HD Camcorder (Model HXR-MC1) with 30 FPS. The curvature of the actuated sample is equal to the inverse radius of curvature, and the radius of curvature was calculated using the following relationships: $l = 2r\sin(\theta/2)$ and $a = r\theta$, where l is the chord length between the tip and base of the bent sample, r is the radius, a is the arc length, and θ is the arc angle.

2.1. Synthesis of 1-(4-vinylbenzyl)imidazole (VBIm)

VBIm was prepared according to a previous literature precedent [47]. $NaHCO_3$ (5.25 g, 62.4 mmol) was added to 100 mL of a binary mixture of water/acetone (1:1 v:v) in a 250 mL two-neck round bottomed flask equipped with an addition funnel and reflux condenser. To this mixture, imidazole (13.61 g, 0.199 mol) was added and stirred until completely dissolved. At room temperature, VBCl (7.61 g, 49.8 mmol) was added drop-wise, after which the solution was heated to 50 °C and stirred for 20 h. Following the reaction, the solid salt remaining was filtered and discarded, and acetone was distilled under reduced pressure at 23 °C. The remaining solution was diluted with 500 mL of diethyl ether, and washed with 50 mL of ultrapure water six times. The organic phase was then washed with 100 mL of 2.0 M HCl three times, saving the aqueous washes. Then, 200 mL of 4.0 M NaOH was added to the acid washes, producing a cloudy heterogeneous solution. This mixture was extracted with 50 mL of diethyl ether three times, the organic phase was dried over anhydrous sodium sulfate, and the ether was removed under reduced pressure at 23 °C. VBIm was isolated as a clear oil that formed pure crystals when dissolved in an equal volume of ethyl acetate and cooled to −20 °C.

2.2. Nitroxide-mediated polymerization VBIm

As an example, VBIm (20.6966 g, 112.3 mmol), $DEPN_2$ (135.6 mg, 0.17 mmol), and DEPN (11.3 mg, 0.03 mmol) were dissolved in DMF (25 mL) and degassed using three freeze–pump–thaw cycles. The flask was back-filled with argon, and heated to 125 °C for 2 h. The solution was cooled to 23 °C, diluted with DMF (20 mL), and precipitated into ethyl acetate. The product was redissolved in methanol and precipitated into diethyl ether. Poly(VBIm) was filtered and dried at reduced pressure (0.5 mmHg) at 40 °C for 18 h.

2.3. Synthesis of poly(EVBIm-Br)

Poly(VBIm) (13.6251 g, 6.67×10^{-5} mol) and 1-bromoethane (82.32 g, 0.755 mol) were dissolved in methanol (100 mL). The solution was purged with argon, and heated to 61 °C for 18 h. The solution was cooled to 23 °C and the product was precipitated into ethyl acetate. Poly(EVBIm-Br) was isolated through filtration and dried at reduced pressure (0.5 mmHg) at 40 °C for 18 h.

2.4. Synthesis of poly(EVBIm-Tf_2N)

Poly(EVBIm-Br) (14.8135 g, 50.5 mmol of repeat unit) and $LiTf_2N$ (72.0395 g, 0.250 mol) were dissolved in separate solution of water

(50 mL each). The solutions were mixed together, immediately forming a white precipitate, and stirred at 23 °C for 24 h. Poly(EVBIm-Tf_2N) was isolated through filtration and dried at reduced pressure (0.5 mmHg) at 40 °C for 18 h.

2.5. Synthesis of poly(Sty-b-[EVBIm][Tf_2N]-b-Sty)

As an example, poly(EVBIm-Tf_2N), (5.0618 g, 9.2×10^{-6} mol), styrene (10.1415 g, 97.3 mmol), and DEPN (4.0 mg, 0.01 mmol) were dissolved in DMF (17.2 mL). The solution was degassed using three freeze–pump–thaw cycles and back-filled with argon. The solution was then heated to 125 °C for 4 h. The solution was cooled to 23 °C, diluted with acetone (50 mL) and precipitated into hexanes. Poly(Sty-*b*-[EVBIm][Tf_2N]-*b*-Sty) was isolated through filtration and dried at reduced pressure (0.5 mmHg) at 40 °C for 18 h. Films of poly(Sty-*b*-[EVBIm][Tf_2N]-*b*-Sty) were cast from a dispersion in acetone (~10 wt%) onto silicon-coated Mylar and annealed at 120 °C for 24 h. Moisture content can significantly influence electromechanical transducers, and therefore feel it is important to stress that the polyelectrolyte central block was anion exchanged to form a hydrophobic polymer in water, and chain extension with styrene resulted in an inherently hydrophobic triblock copolymer. Furthermore, the triblock copolymers were dried extensively near T_g at 0.01 mmHg for 18 h and stored in a desiccator prior to use. Thermogravimetric analysis did not reveal weight loss associated with water.

3. Results and discussion

Nitroxide-mediated polymerization enabled the synthesis of triblock copolymers containing VBIm. Homopolymerization of VBIm using a difunctional nitroxide initiator, $DEPN_2$, with post-polymerization quaternization of the imidazole ring using 1-bromoethane resulted in a water-soluble polyelectrolyte center block precursor. Anion exchange to the Tf_2N^- counteranion in water precipitated a hydrophobic homopolymer. Subsequent chain extension with styrene in a dipolar aprotic solvent resulted in the desired ABA triblock copolymer (Scheme 1). Incorporation of the charged, low T_g imidazolium central block provided an electrochemically stable, highly ion conducting polymer for application in electromechanical transducers. VBIm further enabled controlled radical polymerization through resonance stabilization of the propagating radical, which granted targeted molecular weights. Previous work in our laboratory demonstrated the lack of control for nitroxide-mediated polymerization of vinylimidazole monomers attributed to high rates of propagation and limited radical stability [13]. Polystyrene outer blocks offered mechanically reinforcing phases for suitable mechanical properties. Furthermore, ideal crossover from the styrenic VBIm-based center block precursor to styrene ensured uniform incorporation and triblock copolymer synthesis.

Molecular weight analysis with reaction time revealed a linear dependence in both $\ln([M_0]/[M])$ (Fig. 2a) and conversion (Fig. 2b), where $[M_0]$ is the initial monomer concentration and $[M]$ represents the instantaneous monomer concentration of VBIm. Molecular weight distributions (M_w/M_n) gradually increased upon conversion and reached a constant value of ~1.20. Previous studies reported a necessary post-polymerization functionalization of poly(4-vinylbenzyl chloride) with imidazole to improve control over the polymerization process [32,33,48], however, our investigation clearly demonstrated control over the polymerization of imidazole-functionalized styrenic monomers. Size exclusion chromatography in conjunction with offline refractive index increment measurements determined the absolute weight-average molecular weight (M_w) for the neutral central block precursor was 245,000 g/mol and M_w/M_n of 1.20. ^{1}H NMR spectroscopy determined the ABA triblock copolymer composition through integration of the aromatic resonances relative to the benzylic resonance. Molar ratios obtained from ^{1}H NMR spectroscopy calculated number-average molecular weight (M_n) values for the ABA triblock copolymer (Table 1).

The thermal properties of the center block precursors depended on the presence of charge and counteranion selection (Table 2). T_g increased 41 °C upon quaternization with 1-bromoethane, and the T_g decreased 119 °C following anion exchange to Tf_2N^-. TGA determined that the thermal stability decreased 110 °C upon quaternization due to the mobile basic anion (Br^-) and the ability of the imidazolium ring to serve as a leaving group. Anion exchange from Br^- to a less basic counteranion Tf_2N^- increased thermal stability 99 °C, a trend commonly observed throughout the literature [49]. Mahanthappa and coworkers previously detailed the degradation mechanism for imidazolium poly(VBIm) homopolymers with varying counteranion and alkyl substituent [32]. They determined that Cl^- and BF_4^- counteranions attack the benzyl CH_2 to remove an alkyl-substituted imidazole in a two-step degradation process. In contrast, imidazolium homopolymers with Tf_2N^- counteranions displayed a single-step degradation, which was attributed to main chain polymer degradation.

Two critical parameters for electromechanical transducer fabrication include ionic conductivity and membrane modulus. Poly(Sty-*b*-[EVBIm][Tf_2N]-*b*-Sty) displayed mechanical properties indicative of a microphase-separated triblock copolymer (Fig. 3). DMA confirmed the presence of two distinct polymer phases with the center block T_g at ~26 °C and polystyrene outer block T_g at ~100 °C, which agreed well with DSC results. The sloping plateau region revealed microphase separation between the neutral and ionic block segments. The room temperature modulus of ~100 MPa was ideal for actuator fabrication because this range provides a strong matrix for ion conduction without inhibiting actuation [1,43,44]. Analysis of the elastic modulus determined the bulk triblock copolymer mechanical properties, however analysis of flexural modulus could provide a more suitable connection between mechanical properties and electromechanical transducer performance. Electrochemical impedance spectroscopy determined the temperature-dependent ionic conductivity of poly(Sty-*b*-[EVBIm][Tf_2N]-*b*-Sty) (Fig. 4). Increasing temperature to 150 °C increased ionic conductivity three orders of magnitude, and analysis with the Vogel–Fulcher–Tammann (VFT) equation revealed quality fittings as described later. An upturn in ionic conductivity occurred as the temperature passed through the T_g of polystyrene, causing a small deviation from the predicted VFT behavior ($1000/T \sim 2.75$–2.9 1/K). This observation suggested microphase separation facilitated ion transport through the low T_g ionic phase, while polystyrene external blocks acted as reinforcement to the polymeric membrane increasing integrity. The segmental motion within the ionic phase improved ionic conductivity as polystyrene domains relax with increased temperature. The biphasic design of a microphase-separated triblock copolymer with low T_g ionic domains uniquely promotes ion conduction in concert with robust mechanical properties.

The interplay of ionic conductivity and membrane modulus is critical for electromechanical transducer performance. We observed that as storage modulus decreased two orders of magnitude, ionic conductivity increased two and a half orders of magnitude (Fig. 5). Poly(Sty-*b*-[EVBIm][Tf_2N]-*b*-Sty) displayed an ionic conductivity of $\sim 5.0 \times 10^{-7}$ S/cm when the membrane modulus was 100 MPa. Nafion® displays a hydrated modulus of ~120 MPa and a proton conductivity of 1.1×10^{-1} S/cm [50]. Although seemingly inferior to Nafion®, the adequate ionic conductivity and storage modulus of poly(Sty-*b*-[EVBIm][Tf_2N]-*b*-

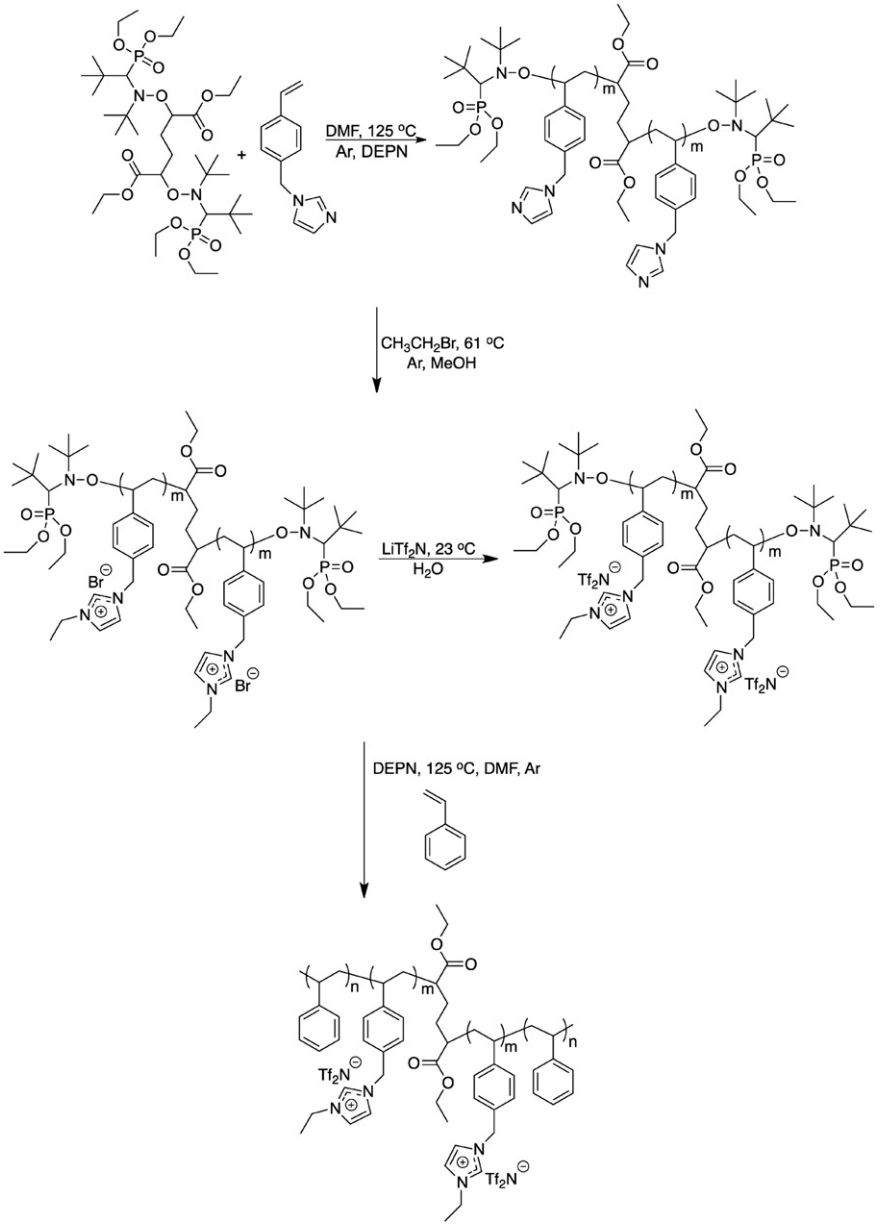

Scheme 1. Synthesis of poly(Sty-*b*-[EVBIm][Tf_2N]-*b*-Sty).

Sty) suggested a candidate for the first cationic membrane incorporated into an electromechanical transducer.

Limited solubility of the final ABA triblock copolymer prevented SEC analysis, and absolute molecular weight and molecular weight distribution remain unknown. While ^{1}H NMR spectroscopy determined the copolymer composition and DMA revealed a microphase-separated physical network, these techniques did not confirm a symmetric ABA triblock copolymer. Probing the copolymer microstructure using small angle X-ray scattering (SAXS) and transmission electron microscopy (TEM) indicated a phase-separated morphology without long-range order (see Electronic Supplementary Information). Large, irregular microdomains in TEM suggested the presence of central block homopolymer and/or diblock copolymers in addition to symmetric ABA triblock copolymers; a lack of scattering peaks in SAXS is consistent with the large interdomain distances in TEM. The presence of homopolymer central block and diblock copolymers limited the long-range order of the microphase separation, and prevented precise microstructure formation. However, the microphase-separated copolymer exhibited a sufficient modulus and ionic conductivity to warrant investigation as the conducting membrane in electromechanical transducers.

An ideal membrane modulus and suitable ionic conductivity prompted the incorporation of poly(Sty-*b*-[EVBIm][Tf_2N]-*b*-Sty) into an electromechanical transducer. Application of the layer-by-layer CNC provided intimate contact between the polymeric membrane and exterior gold electrodes [43]. Heflin, Zhang and coworkers prepared electromechanical transducers with a Nafion® ionomeric membrane and poly(allylamine hydrochloride)/anionic gold nanoparticle or RuO_2 CNCs [43,44]. They showed that the layer-by-layer direct assembly method provided precise control over the CNC thickness and improved actuation speed and strain production. For the present work, a poly(Sty-*b*-[EVBIm][Tf_2N]-*b*-Sty) membrane of 50 μm thickness was coated with a 30-bilayer CNC consisting of poly(allylamine hydrochloride) and 3 nm anionic gold nanoparticles. A 4 V applied potential at ambient conditions

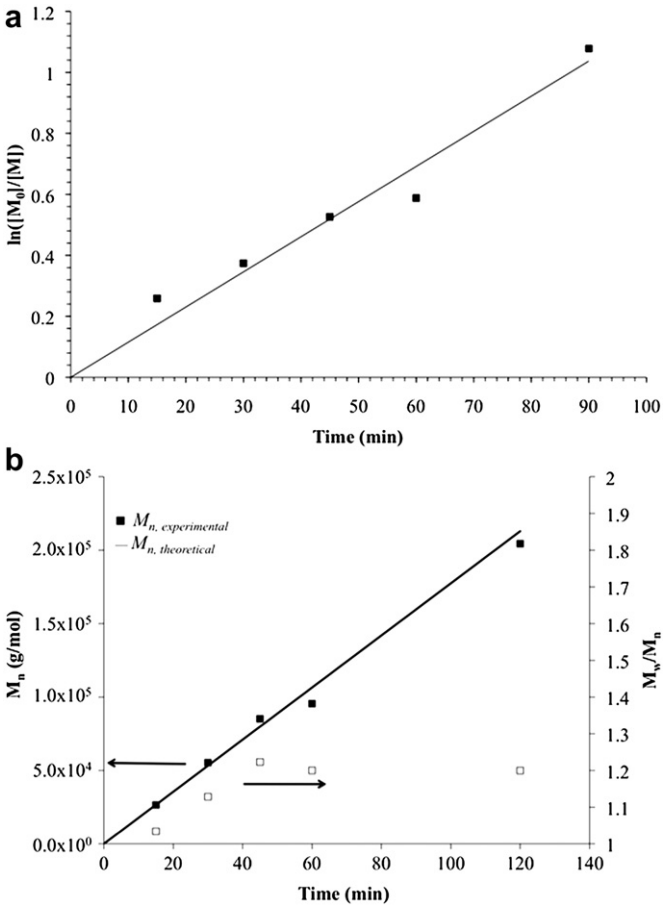

Fig. 2. Analysis of the living nature of poly(VBIm) prepared using nitroxide-mediated polymerization, plots of (a) pseudo-first-order kinetics and (b) M_n and M_w/M_n versus time. [M_0] and [M] represent the initial and instantaneous monomer concentrations, respectively.

(23 °C and ~43% RH) induced electromechanical actuation, and mechanical deformation increased up to 60 s (Fig. 6). A common feature of electroactive devices is ion saturation at the oppositely charged electrode, which reverses the polarity of the device. The reversed polarity causes ion migration in the opposite direction of the applied potential and the device relaxes [1,7,51]. Device relaxation was absent for poly(Sty-*b*-[EVBIm][Tf_2N]-*b*-Sty), which indicated ion migration and accumulation at one electrode without reverse migration.

Actuator curvature is the inverse of the deformed membrane's radius of curvature, which increased with longer exposure to the applied potential (Fig. 7). Application of an equivalent CNC to a Nafion® membrane of equal thickness (50 μm) served as a control. Nafion® exhibited a similar curvature up to 20 s, after which

Table 1
Number-average and weight-average molecular weights and molecular weight distributions for center block homopolymers and the subsequent triblock copolymer.

Sample	M_n(kg/mol)	M_w(kg/mol)	M_w/M_n
Poly(VBIm)	204[a]	245	1.20
Poly(EVBIm-Br)	325[b]	ND	ND
Poly(EVBIm-Tf_2N)	546[b]	ND	ND
Poly(Sty-*b*-[EVBIm][Tf_2N]-*b*-Sty)	804[b]	ND	ND

[a] Absolute M_w determined with aqueous SEC and offline d*n*/d*c* measurement.
[b] ^{1}H NMR spectroscopy, ND = none determined.

Table 2
Glass transition and degradation temperatures for the center block homopolymers.

Sample	T_g (°C)[a]	$T_{D,5\%}$ (°C)[b]
Poly(VBIm)	107	354
Poly([EVBIm][Br])	148	244
Poly([EVBIm][Tf_2N])	29	343

[a] DSC, 10 °C/min heating ramp, $N_2$2nd heat.
[b] TGA, 10 °C/min heating ramp, N_2.

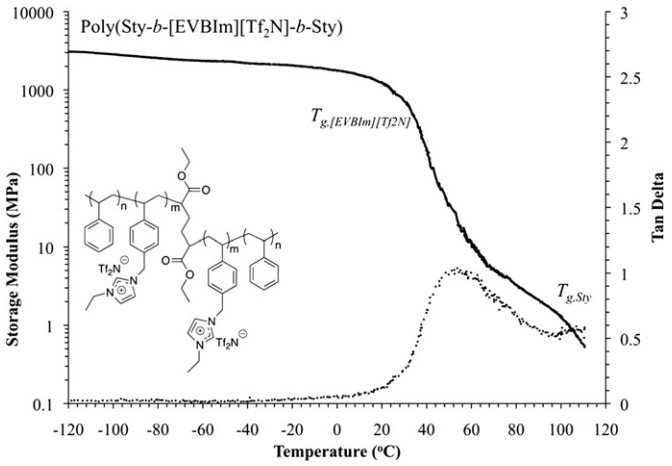

Fig. 3. DMA determined the mechanical properties of poly(Sty-*b*-[EVBIm][Tf_2N]-*b*-Sty) at a temperature ramp of 3 °C/min and a frequency of 1 Hz.

actuation ceased while the poly(Sty-*b*-[EVBIm][Tf_2N]-*b*-Sty) electromechanical transducer displayed final curvature 2.5 times larger than Nafion®. Both poly(Sty-*b*-[EVBIm][Tf_2N]-*b*-Sty) and Nafion® electromechanical transducers without the CNC displayed curvatures 4 times lower than those with the CNC. However, the poly(Sty-*b*-[EVBIm][Tf_2N]-*b*-Sty) electromechanical transducer again displayed curvature 2.5 times larger than Nafion®. The ion clusters of Nafion® likely hydrated at ambient conditions or during the CNC application process to facilitate ion transport. Conversely, the hydrophobic nature of the ionic phase in poly(Sty-*b*-[EVBIm][Tf_2N]-*b*-Sty) would likely prevent moisture uptake. The performance of poly(Sty-*b*-[EVBIm][Tf_2N]-*b*-Sty) in a dry and non-diluted state relative to Nafion® is particularly attractive for future technologies. Recent studies incorporated poly(*t*-butyl Sty-*b*-ethylene-

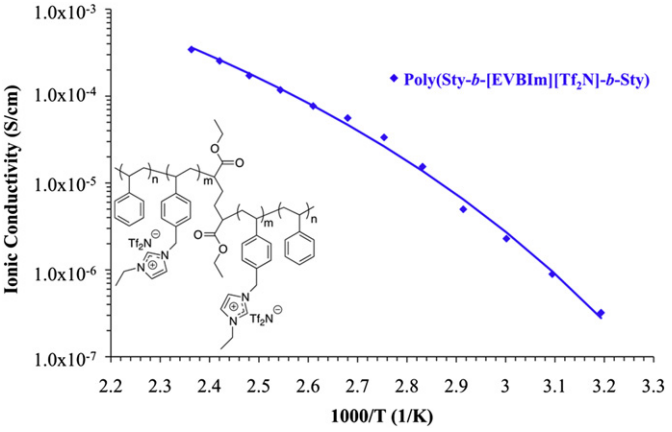

Fig. 4. Temperature-dependent ionic conductivity of poly(Sty-*b*-[EVBIm][Tf_2N]-*b*-Sty), the solid line represents regression of the conductivity data with the VFT equation.

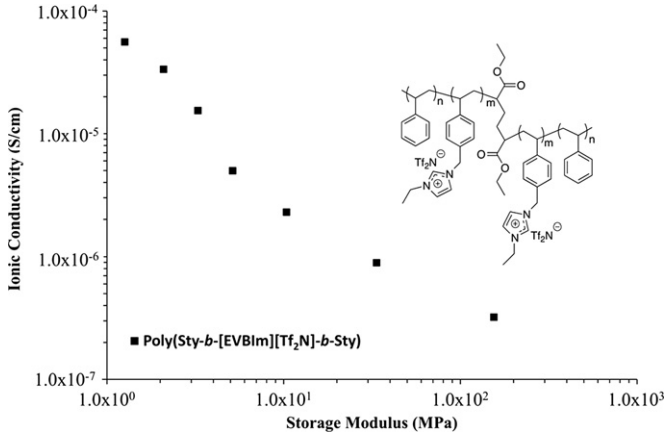

Fig. 5. Ionic conductivity plotted versus storage modulus. EIS determined the ionic conductivity and DMA determined the storage modulus.

co-propylene-*b*-sulfonated Sty-*b*-ethylene-*co*-propylene-*b*-*t*-butyl Sty) pentablock copolymer into electromechanical transducers [52,53]. Spontak and coworkers quantified actuation using L/R, where L is the film length and R is the radius of curvature, and observed a value of ~4.5 and ~3.2 after 25 min of a 7 and 9 V applied potential, respectively [52]. Poly(Sty-*b*-[EVBIm][Tf_2N]-*b*-Sty) displayed a L/R value of 3.2 after 1.33 min of a 4 V applied potential. In comparison, the electromechanical transducers studied herein exhibited similar curvatures at lower voltages and actuation times.

Leo and coworkers extensively studied the performance of Nafion®-based electromechanical transducers and revealed critical parameters for optimizing their performance. First, the strain generated from the applied voltage directly relates to the capacitance of the ionomeric membrane [50]. Simulations and experimental investigations further revealed that the permittivity of the ionomeric membrane decreased the charging time of the ionomer–electrode interface and increased charge density accumulation at the electrodes [54]. Enhanced diffusion through the ionomeric membrane decreased the charging time of the ionomer–electrode interface and increased current production without affecting the charge density accumulation [54]. Simulations also revealed that an increased percentage of conductive nanoparticles in the CNC increased the charge density accumulation at the interface between the ionomer and the electrode [55]. These investigations showed that the charge accumulation at the ionomer–electrode interface dominated the strain generation in Nafion®-based electromechanical transducers and provided key parameters to tailor the ionomer and CNC properties.

These previous investigations revealed information that directly pertains to the triblock copolymer investigated herein. The weakly coordinating Tf_2N^- counteranions in the poly(Sty-*b*-[EVBIm][Tf_2N]-*b*-Sty) triblock copolymer participated in ion conduction through the ion-hopping mechanism, similar to findings from Leo and coworkers [26]. The high charge content and mobile Tf_2N^- counterion promoted charge accumulation at the ionomer–electrode interface and subsequent mechanical deformation. Furthermore, the relative permittivity of the ionic phases in the triblock copolymer were presumably higher than those of the Nafion® ion clusters based on their relative performances. Ionomers have significantly higher relative permittivity values (ε_r), potentially on the order of 10^9–10^{10} [50]. The combination of weakly associated counteranions, high ionic phase relative permittivity, and high nanoparticle vol% in the CNC facilitated charge accumulation at the ionomer–electrode interface and superior performance compared to Nafion®. These individual advantages worked in concert for poly(Sty-*b*-[EVBIm][Tf_2N]-*b*-Sty) as a cationic triblock copolymer incorporated into an electromechanical transducer.

Recent studies show that the addition of IL dramatically influences the mechanical properties, ionic conductivity, and morphology of polymeric membranes [26,56,57]. The addition of the IL, [EMIm][TfO], decreased the T_g of the ionic center block

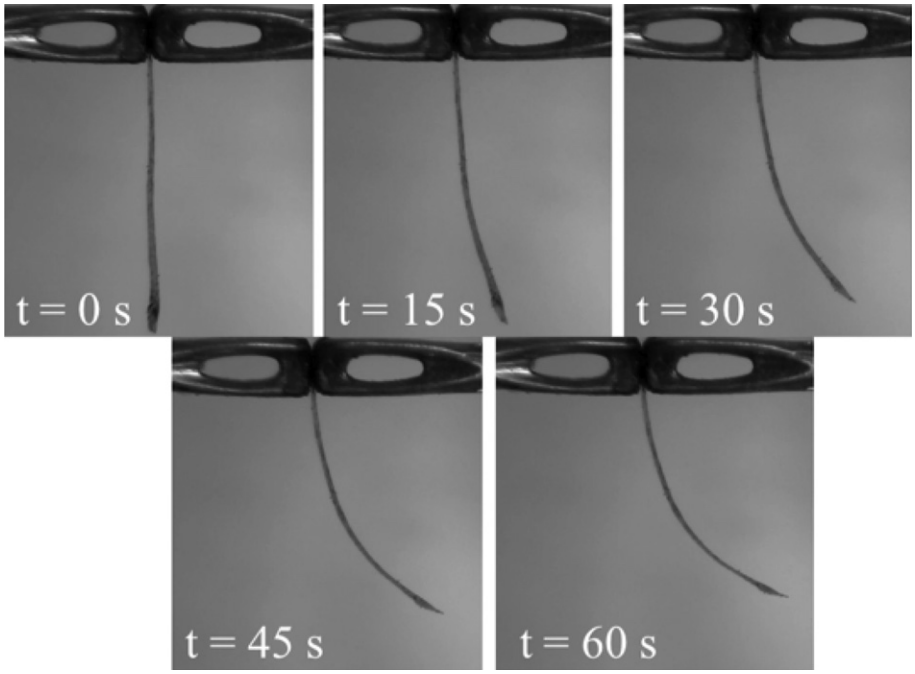

Fig. 6. Still images of electromechanical transducers fabricated from poly(Sty-*b*-[EVBIm][Tf_2N]-*b*-Sty), a poly(allylamine hydrochloride)/anionic gold nanoparticle CNC, and gold electrodes under an applied potential of 4 V.

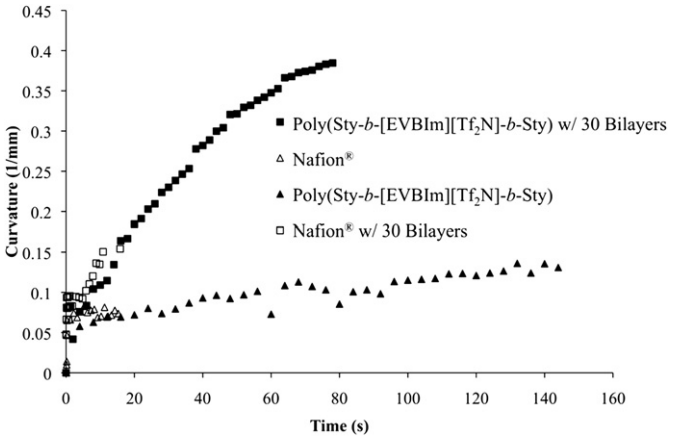

Fig. 7. Curvature observed for electromechanical transducers under a 4 V applied voltage (+) with and without CNC application.

(Table 3). A cast-with method ensured uniform incorporation of the IL throughout the triblock copolymers. Long and coworkers recently showed that the method of IL incorporation impacted the mechanical properties, conductivities, and morphologies of the polymer matrix [56,57]. Solution cast films from acetone with 0, 20, and 40 wt% IL displayed decreased center block T_g's with increased IL content; the T_g decreased 15 °C and 50 °C at 20 and 40 wt% IL, respectively. Importantly, the T_g of the polystyrene outer blocks did not change, which indicated selective incorporation of the IL into the ionic center block. Long and coworkers recently showed that ILs selectively swell ionic domains in microphase-separated polymers using X-ray scattering and DMA [56].

Electrochemical impedance spectroscopy determined the temperature-dependent ionic conductivity of the triblock copolymers with 0, 20, and 40 wt% [EMIm][TfO] (Fig. 8a). Higher IL levels increased ionic conductivity an order of magnitude from 0 < 20 < 40 wt% IL. Ionic conductivity for the polymeric membranes were 0.3, 3.4, and 17.4 mS/cm with 0, 20, and 40 wt% IL at 150 °C. Normalization of temperature with T_g (T_g/T) collapsed the temperature-dependent ionic conductivity of the IL-incorporated triblock copolymers onto a single curve, while the neat triblock copolymer membrane displayed an ionic conductivity an order of magnitude lower (Fig. 8b). Leo and coworkers discussed the mechanism of ion conduction for IL-swollen Nafion® membranes, where the IL imidazolium cation exchanged with lithium, potassium, cesium, or tetraethylammonium countercations of the Nafion® ion clusters freeing the cations to migrate [26]. Larger countercations were loosely bound and displayed higher actuation speeds at lower levels of IL. The added IL in poly(Sty-*b*-[EVBIm][Tf_2N]-*b*-Sty) increased free ion content and ion mobility, which increased ionic conductivity. The Tf_2N^- counteranions on the polymer are similar to the TfO^- counteranions in the IL. Therefore, counteranion displacement remains negligible. The increased ionic conductivity for IL-incorporated triblock copolymers related to the increased ion concentration and plasticization due to added diluent.

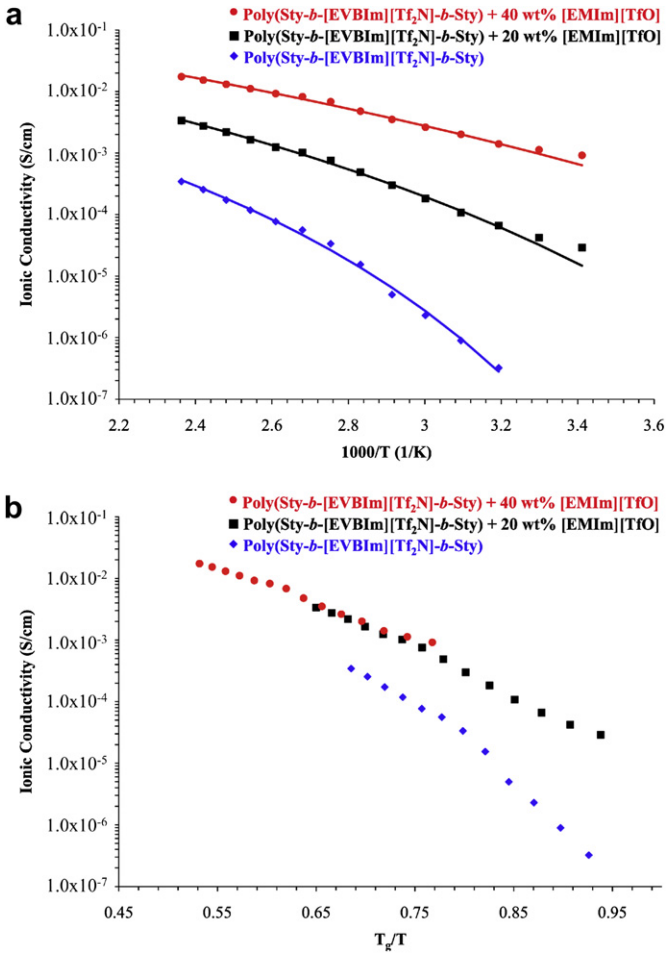

Fig. 8. Temperature-dependent ionic conductivity of poly(Sty-*b*-[EVBIm][Tf_2N]-*b*-Sty) with 0, 20, and 40 wt% [EMIm][TfO] plotted versus (a) 1000/*T* and (b) T_g/T. Solid lines indicate analysis using the VFT equation.

Analysis of the ionic conductivity using the VFT equation (eq. (1)) revealed important information regarding the structure–conductivity relationship. In this equation, σ_∞ is the infinite temperature conductivity, $-B$ is a fitting parameter, and T_0 is the Vogel temperature where ion motion first occurs [58–60]. The infinite temperature conductivity increased directly with IL addition, and the Vogel temperature decreased with a decrease in T_g (Table 4). Plasticization of the polymeric membrane from the addition of the IL reduced the Vogel temperature and promoted ion conduction at lower temperatures. As the concentration of IL

Table 3
Thermal analysis of triblock copolymers with 0, 20, and 40 wt% [EMIm][TfO].

Sample	[EMIm][TfO] (wt%)	$T_{g,1}$ (°C)[a]	$T_{g,2}$ (°C)[a]	$T_{D,5\%}$ (°C)[b]
Poly(Sty-*b*-[EVBIm][Tf_2N]-*b*-Sty)	0	17	107	341
	20	2	106	367
	40	−48	107	375

[a] DSC, 10 °C/min, $N_2$2nd heat.
[b] TGA, 10 °C/min, N_2.

Table 4
VFT-fitting parameters obtained for temperature-dependent ionic conductivities of poly(Sty-*b*-[EVBIm][Tf_2N]-*b*-Sty).

Sample	[EMIm][TfO] (wt%)	*B* (K)[a]	σ_∞ (S/cm)[b]	T_0 (K)[c]	$T_{g,DSC}$ (K)[d]
Poly(Sty-*b*-[EVBIm][Tf_2N]-*b*-Sty)	0	1400	0.271	212	290
	20	1400	0.780	164	275
	40	1390	1.750	117	225

[a] VFT activation energy.
[b] infinite temperature conductivity.
[c] Vogel temperature.
[d] DSC, 10 °C/min, 2nd heat, N_2.

increased, the infinite temperature conductivity also increased, as infinite temperature conductivity directly relates to the number density of ions [61].

$$\sigma = \sigma_\infty \left(\frac{-B}{T - T_0} \right) \quad (1)$$

The addition of IL reduced the storage modulus of poly(Sty-*b*-[EVBIm][Tf_2N]-*b*-Sty) below a suitable value for electromechanical transducer fabrication. However, it provided critical information for the design of future ionomeric triblock copolymers. The poly(Sty-*b*-[EVBIm][Tf_2N]-*b*-Sty) triblock copolymer studied herein provides a roadmap for the parameters of future polymeric membranes, i.e., charge placement in low T_g ionic center blocks, control of molecular weight, a poly(EVBIm-Tf_2N) center block precursor that provides high ionic conductivity and low T_g, threshold compositions for suitable moduli, a compatible CNC that maximizes performance, and the influence of IL on ionic conductivity and T_g. Future studies that develop a relationship between morphology and ion conduction in well-defined ionomeric triblock copolymers will generate feedback on polymer structure and performance. Analysis of triblock copolymer compositions that maintain suitable moduli upon IL loading will expand the library of polymeric membranes available for incorporation into electromechanical transducers.

4. Conclusion

We prepared the first electromechanical transducer incorporating a cationic triblock copolymer using poly(Sty-*b*-[EVBIm][Tf_2N]-*b*-Sty). Nitroxide-mediated polymerization of VBIm controlled molecular weight and molecular weight distribution (204,000 g/mol with M_w/M_n of 1.20). Chain extension of the ionic poly(EVBIm-Tf_2N) center block precursor with styrene prepared the ABA triblock copolymer. DMA revealed a modulus suitable for electromechanical transducer fabrication, approximately 100 MPa at 23 °C. Comparison of ionic conductivity to membrane modulus revealed that decreased modulus resulted in significantly increased ionic conductivity, with conductivities of approximately 5.0×10^{-7} S/cm at a membrane modulus of 100 MPa. Actuator testing showed device final curvatures over double those achieved with Nafion®, both with and without the added CNC. Incorporation of [EMIm][TfO] increased ionic conductivity approximately an order of magnitude upon addition of 20 wt% and an additional order of magnitude for 40 wt% IL. A free-standing film of the 40 wt% IL-incorporated poly(Sty-*b*-[EVBIm][Tf_2N]-*b*-Sty) displayed an ionic conductivity approaching 20 mS/cm at 150 °C. VFT analysis indicated reduced Vogel temperatures and increased infinite temperature conductivities despite similar activation energies. Triblock copolymers incorporating imidazolium functionality exhibited tunable physical, thermal, electrical, and mechanical properties, successfully enabled the fabrication of a functioning electromechanical transducer, and displayed tremendous potential as electroactive devices.

Acknowledgement

The authors wish to acknowledge Dr. Andy Sarles for help with EIS data interpretation. This material is based upon work supported by the U.S. Army Research Office under grant number W911NF-07-1-0452 Ionic Liquids in Electro-Active Devices (ILEAD) MURI. We acknowledge the Institute for Critical Technology and Applied Science (ICTAS) for funding the acquisition of instrumentation used in this research. This material is based upon work supported by the Army Research Office (ARO) under Award No. W911NF-10-1-0307.

Appendix A. Supplementary material

Supplementary data related to this article can be found in the online version at doi:10.1016/j.polymer.2012.06.023.

References

[1] Duncan AJ, Leo DJ, Long TE. Macromolecules 2008;41(21):7765–75.
[2] Tudryn GJ, Liu W, Wang S-W, Colby RH. Macromolecules 2011;44(9):3572–82.
[3] Wang S-W, Liu W, Colby RH. Chemistry of Materials 2011;23(7):1862–73.
[4] Akle B, Bennett M, Leo D, Wiles K, McGrath J. Journal of Materials Science 2007;42(16):7031–41.
[5] Akle BJ, Leo DJ. Smart Materials and Structures 2007;16(4):1348.
[6] Montazami R, Liu S, Liu Y, Wang D, Zhang Q, Heflin JR. Journal of Applied Physics 2011;109(10):104301–5.
[7] Nemat-Nasser S, Jiang Yu L. Journal of Applied Physics 2000;87(7):3321.
[8] Weiland LM, Leo DJ. Smart Materials and Structures 2004;13(2):323.
[9] Lin J, Liu Y, Zhang QM. Polymer 2011;52(2):540–6.
[10] Duncan AJ, Layman JM, Cashion MP, Leo DJ, Long TE. Polymer International 2009;59(1):25–35.
[11] Eisenberg A, Hird B, Moore RB. Macromolecules 1990;23(18):4098–107.
[12] Mauritz KA, Moore RB. Chemical Reviews 2004;104(10):4535–86.
[13] Green MD, Allen Jr MH, Dennis JM, DS-dl Cruz, Gao R, Winey KI, et al. European Polymer Journal 2011;47(4):486–96.
[14] Cheng S, Beyer FL, Mather BD, Moore RB, Long TE. Macromolecules 2011;44(16):6509–17.
[15] Green MD, Long TE. Polymer Reviews 2009;49(4):291–314.
[16] Rogers RD. Nature 2007;447(7147):917–8.
[17] Smiglak M, Metlen A, Rogers RD. Accounts of Chemical Research 2007;40(11):1182–92.
[18] Fannin AA, Floreani DA, King LA, Landers JS, Piersma BJ, Stech DJ, et al. The Journal of Physical Chemistry 1984;88(12):2614–21.
[19] Wilkes JS. Green Chemistry 2002;4(2):73–80.
[20] Wilkes JS, Zaworotko MJ. Journal of the Chemical Society, Chemical Communications 1992;13:965–7.
[21] Yoshizawa M, Narita A, Ohno H. Australian Journal of Chemistry 2004;57(2):139–44.
[22] Ogihara W, Washiro S, Nakajima H, Ohno H. Electrochimica Acta 2006;51(13):2614–9.
[23] Ye Y, Elabd YA. Polymer 2011;52(5):1309–17.
[24] Marcilla R, Blazquez JA, Rodriguez J, Pomposo JA, Mecerreyes D. Journal of Polymer Science Part A: Polymer Chemistry 2004;42(1):208–12.
[25] Chen H, Choi J- H, Salas-de la Cruz D, Winey KI, Elabd YA. Macromolecules 2009;42(13):4809–16.
[26] Bennett MD, Leo DJ, Wilkes GL, Beyer FL, Pechar TW. Polymer 2006;47(19):6782–96.
[27] Bennett MD, Leo DJ. Sensors and Actuators A: Physical 2004;115(1):79–90.
[28] Akle BJ, Bennett MD, Leo DJ. Sensors and Actuators A: Physical 2006;126(1):173–81.
[29] Liu S, Liu W, Liu Y, Lin J-H, Zhou X, Janik MJ, et al. Polymer International 2010;59(3):321–8.
[30] Yang L, Sheng L, Junhong L, Dong W, Jain V, Montazami R, et al. Applied Physics Letters 2010;96(22):223503.
[31] Green MD, Salas-de la Cruz D, Ye Y, Layman JM, Elabd YA, Winey KI, et al. Macromolecular Chemistry and Physics 2011;212(23):2522–8.
[32] Weber RL, Ye Y, Banik SM, Elabd YA, Hickner MA, Mahanthappa MK. Journal of Polymer Science Part B: Polymer Physics 2011;49(18):1287–96.
[33] Weber RL, Ye Y, Schmitt AL, Banik SM, Elabd YA, Mahanthappa MK. Macromolecules 2011;44(14):5727–35.
[34] Zhang S, Lee KH, Frisbie CD, Lodge TP. Macromolecules 2011;44(4):940–9.
[35] Shankar R, Ghosh TK, Spontak RJ. Soft Matter 2007;3(9):1116–29.
[36] Krishnan AS, Vargantwar PH, Ghosh TK, Spontak RJ. Journal of Polymer Science Part B: Polymer Physics 2011;49(22):1569–82.
[37] Shankar R, Ghosh TK, Spontak RJ. Advanced Materials 2007;19(17):2218–23.
[38] Shankar R, Ghosh TK, Spontak RJ. Macromolecular Rapid Communications 2007;28(10):1142–7.
[39] Shankar R, Ghosh TK, Spontak RJ. Sensors and Actuators A: Physical 2009;151(1):46–52.
[40] Shankar R, Krishnan AK, Ghosh TK, Spontak RJ. Macromolecules 2008;41(16):6100–9.
[41] Vargantwar PH, Brelander SM, Krishnan AS, Ghosh TK, Spontak RJ. Applied Physics Letters 2011;99(24):242901.
[42] Vargantwar PH, Özçam AE, Ghosh TK, Spontak RJ. Advanced Functional Materials 2012;22(10):2100–13.
[43] Liu S, Montazami R, Liu Y, Jain V, Lin M, Zhou X, et al. Sensors and Actuators A: Physical 2010;157(2):267–75.
[44] Liu S, Montazami R, Yang L, Jain V, Minren L, Heflin JR, et al. Applied Physics Letters 2009;95(2):023505.
[45] Grimaldi S, Finet J-P, Le Moigne F, Zeghdaoui A, Tordo P, Benoit D, et al. Macromolecules 2000;33(4):1141–7.
[46] Mather BD, Baker MB, Beyer FL, Berg MAG, Green MD, Long TE. Macromolecules 2007;40(19):6834–45.

[47] Miyake T, Takeda K, Tada K. Novel basic imidazolylmethylstyrene compound, its polymer, a process for the preparation thereof and a use as ion exchange resin. United States: Asahi Kasei Kogyo Kabushiki Kaisha (Osaka, JP); 1984.
[48] Stancik CM, Lavoie AR, Schutz J, Achurra PA, Lindner P, Gast AP, et al. Langmuir 2004;20(3):596–605.
[49] Hunley MT, England JP, Long TE. Macromolecules 2010;43(23):9998–10005.
[50] Akle BJ, Leo DJ, Hickner MA, McGrath JE. Journal of Materials Science 2005; 40(14):3715–24.
[51] Asaka K, Oguro K. Journal of Electroanalytical Chemistry 2000;480(1–2): 186–98.
[52] Vargantwar PH, Shankar R, Krishnan AS, Ghosh TK, Spontak RJ. Soft Matter 2011;7(5):1651–5.
[53] Gao R, Wang D, Heflin JR, Long TE. Journal of Materials Chemistry 2012.
[54] Wallmersperger T, Akle BJ, Leo DJ, Kr√∂plin B. Composites Science and Technology 2008;68(5):1173–80.
[55] Akle BJ, Habchi W, Wallmersperger T, Akle EJ, Leo DJ. Journal of Applied Physics 2011;109(7):074509.
[56] Brown RH, Duncan AJ, Choi J-H, Park JK, Wu T, Leo DJ, et al. Macromolecules 2009;43(2):790–6.
[57] Wu T, Beyer FL, Brown RH, Moore RB, Long TE. Macromolecules 2011;44(20): 8056–63.
[58] Vogel H. Physikalische Zeitschrift 1921;22:645–6.
[59] Fulcher GS. Journal of the American Ceramic Society 1925;8(6):339–55.
[60] Tammann G. Zeitschrift für Anorganische und Allgemeine Chemie 1926; 156(1):245–57.
[61] Sangoro JR, Serghei A, Naumov S, Galvosas P, Karger J, Wespe C, et al. Physical Review E 2008;77(5):4.